Theoretical prediction of multiferroicity in double perovskite Y_2NiMnO_6

Sanjeev Kumar,[1,2,3] Gianluca Giovannetti,[4] Jeroen van den Brink,[3] and Silvia Picozzi[4]
[1]*Institute Lorentz for Theoretical Physics, Leiden University, 2300 RA Leiden, The Netherlands*
[2]*Faculty of Science and Technology, University of Twente, P.O. Box 217, 7500 AE Enschede, The Netherlands*
[3]*Institute of Theoretical Solid State Physics, IFW Dresden, 01171 Dresden, Germany*
[4]*Consiglio Nazionale delle Ricerche-Istituto Nazionale per la Fisica della Materia (CNR-INFM), CASTI Regional Laboratory, 67100 L'Aquila, Italy*

(Received 13 November 2009; revised manuscript received 3 May 2010; published 18 October 2010)

We put forward double perovskites of the R_2NiMnO_6 family (with R a rare-earth atom) as a distinct class of multiferroics on the basis of *ab initio* density-functional calculations. We show that changing R from La to Y drives the ground state from ferromagnetic to antiferromagnetic with $\uparrow\uparrow\downarrow\downarrow$ spin patterns. This E^*-type ordering breaks inversion symmetry and generates a ferroelectric polarization of few microcoulomb per square centimeter. By analyzing a model Hamiltonian, we understand the microscopic origin of this transition and show that an external electric field can be used to tune the transition, thus allowing electrical control of the magnetization.

DOI: 10.1103/PhysRevB.82.134429 PACS number(s): 75.80.+q, 71.45.Gm, 71.10.Ca, 73.21.−b

I. INTRODUCTION

Materials with simultaneous magnetic and ferroelectric ordering—multiferroics—are attracting enormous scientific interest due to their potential for applications in memory and data storage devices.[1,2] Multiferroics with magnetically induced ferroelectric order are particularly interesting due to their strong magnetoelectric coupling, which is required for an electric (magnetic) control of magnetic (electric) order parameter: a very desirable property from a technological point of view.[3] Therefore, the search for new multiferroics with the ferroelectric order driven by the magnetic order is currently a very active and important field of research.

Although the term "multiferroic" has become popular only in the last decade, the topic of simultaneous existence of ferroelectricity and magnetism in solids is not new.[4–6] It was realized early on that the order parameters for the ferroelectric and ferromagnetic (FM) order are often chemically incompatible.[7] The possibility of magnetoelectric coupling in Cr_2O_3 was predicted by Dzyaloshinskii and confirmed later by Astrov.[8,9] In addition, the existence of weak ferromagnetism induced by ferroelectric polarization in $BaMnF_4$ was shown by Fox and Scott.[10,11] More recently, a large number of discovered multiferroics belong to the class where a ferroelectric order is induced by a nontrivial magnetic state. The possibility to design novel materials where ferromagnetism can be induced by the interplay between polarization and Dzyaloshinskii-Moriya interaction has been suggested recently.[12] Finally, many Pb- and Fe-based compounds have also been proposed as potential multiferroics.[13–16]

In this paper, we show, by using first-principles density-functional theory (DFT) calculations and a model Hamiltonian analysis, that the magnetic order in the double-perovskite compounds R_2NiMnO_6 (RNMO) changes from ferromagnetic for R=La and Sm to the E^*-type for R=Y. The E^*-type magnetic structure consists of $\uparrow$-$\uparrow$-$\downarrow$-$\downarrow$ spin chains along the *cubic* perovskitelike directions (see Fig. 3), or equivalently, zigzag FM spin chains antiferromagentically coupled in-plane to the neighboring zigzag chain, with an out-of-plane FM coupling.[17] E^*-type magnetism breaks inversion symmetry and thus allows a ferroelectric polarization to occur. We will show using Berry-phase (BP) approach that indeed Y_2NiMnO_6 is multiferroic with a electric polarization of few microcoulomb per square centimeter. We will show that vice versa the magnetic transition from ferro to E^*-type can be tuned by an external electric field, thus allowing electric control of the ferromagnetic order parameter. The E^* spin configuration, together with the checkerboard arrangement of Ni^{2+}-Mn^{4+} ions leads to inversion-symmetry breaking and gives rise to a ferroelectric polarization in Y_2NiMnO_6, which we explicitly compute using DFT methods. To the best of our knowledge, Y_2NiMnO_6 (YNMO) and Sm_2NiMnO_6 (SNMO) have never been synthesized. Therefore, our work goes into the direction of first-principles materials design, aimed at achieving multiferroicity in advanced compounds by tuning their chemical composition and, in turn, their structural, ferroelectric and magnetic properties.

The rest of the paper is organized as follows: in Sec. II, we discuss the details of the computational *ab initio* method. The results of DFT calculations are presented in Sec. III. A model Hamiltonian analysis, with the essential parameters taken from the DFT results, is presented in Sec. IV. Section V is devoted to the results on ferroelectric polarization using the Berry-phase approach and a discussion, and conclusions are presented in Sec. VI.

II. COMPUTATIONAL METHOD

The double perovskite La_2NiMnO_6 (LNMO) is a ferromagnetic insulator with a Curie temperature close to room temperature ($T_c \sim 280$ K). The structure of LNMO changes from rhombohedral ($R\bar{3}$) at high temperature, to monoclinic with $P2_1/n$ symmetry group at low temperature.[18,19] DFT has been successful in understanding the FM insulating behavior and the dielectric anomalies observed experimentally in LNMO.[20,21] We work in the framework of density-functional theory, using the Vienna *ab initio* simulation package,[22] in which the Kohn-Sham equations are computed

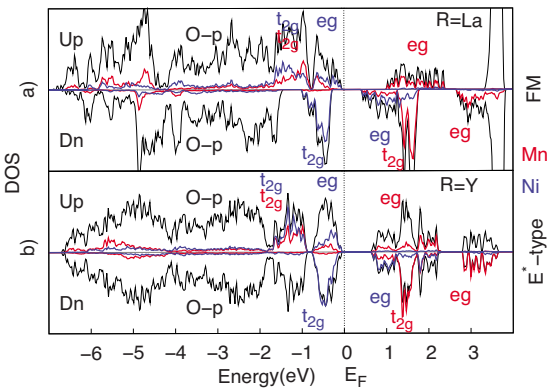

FIG. 1. (Color online) (a) Density of states in $P2_1/n$ symmetry for FM-type magnetic structure in LNMO; (b) density of states in $P2_1$ symmetry for E*-type magnetic structure in YNMO. Zero energy is set to be Fermi level.

using the projector-augmented wave method and solved describing electronic exchange and correlation in the generalized gradient approximation (GGA), using the functional introduced by Perdew, Burke, and Ernzerhof (PBE).[23] The plane-wave cutoff was chosen as 400 eV. A [3,6,5] mesh was used for the Brillouin-zone sampling. In the BP approach, we integrated over strings parallel to a,b,c axes, each of them divided in eight k points. Self-consistent calculations and structural relaxations were iterated until a convergence criteria of 0.01 meV was reached. No symmetry constraints were imposed during the relaxation.

III. DFT RESULTS

The spin-resolved density of states (DOS) of LNMO is shown in Fig. 1(a) and they agree well with the one in Ref. 20. The octahedral surrounding of Mn and Ni atoms split the Mn $3d$ and Ni $3d$ manifolds into the t_{2g} and e_g levels. In the spin-up channel, the Ni t_{2g} and Ni e_g are found within the range of 2 eV below the Fermi level (E_F) mixed with O $2p$ and the Mn t_{2g} states, the latter being localized between the Ni t_{2g} and the Ni e_g. The Mn e_g remain empty, separated by ~2.5 eV from the Mn t_{2g}. In the down-spin channel the Ni t_{2g} states are located between the O $2p$ and the Fermi level while the Ni e_g lie above the Fermi level along with the Mn t_{2g} and the Mn e_g. This distribution of states corresponds to the nominal valences Ni^{2+} (d^8) and Mn^{4+} (d^3): the magnetic moments in our simulations are indeed found to be 1.4 μ_B and 2.9 μ_B, respectively, close to the experimental values.[24]

Calculating the DFT total energies of the different magnetic structures on the relaxed crystal structure of LNMO and using a least-squares mean method to fit their values by an effective Heisenberg Hamiltonian (as in Ref. 25), we extract the magnetic couplings J_{ij}. Note that the spin-orbit coupling, which is not included here, might change slightly the values of J_{ij} (see Ref. 20).

Experimentally, the unit-cell parameters of double perovskites R_2NiMnO_6 with R=Sm and Y are unknown. Since the theoretical lattice parameters of LNMO obtained within GGA are very close to the experimental estimates (see also Ref. 20), we infer a good accuracy for the prediction of structural properties. Therefore, we determine the lattice parameters and the internal coordinates of the ions for R=Sm and Y by carrying out the first-principles volume and shape optimization for the monoclinic phases upon imposing a FM spin configuration. The PBE theorethical lattice parameters are for R=Sm: a=5.309 Å, b=5.513 Å, c=7.574 Å, β=90.218°, for R=Y: a=5.239 Å, b=5.490 Å, c=7.494 Å, β=90.437°. Our results may provide basis to refine the crystallographic structures experimentally. A general trend is found: a smaller size of the radius of the rare earth is such to decrease the Ni-O-Mn angles increasing the octahedral distortions, which in turn reduces the effective interactions between Ni and Mn ions. Following this procedure, the total energies of different magnetic structures as considered above for R=La reveal a transition from a FM (for R=La,Sm) to the E*-type magnetic structure (for smaller rare-earth ions R=Y).[26] RNMO with R=Sm and Y are found to be insulators with electronic structures very close to that of LNMO. We show in Fig. 1(b) the spin-resolved DOS of YNMO in the E*-type magnetic structure. Small differences are found in the values of the band gaps and magnetic moments at Ni and Mn sites between the considered magnetic structures in all RNMO studied in this work. The magnetism is governed by the superexchange interactions due to the Hund's rule and energy gain allows virtual hopping of parallel spins and forbids antialigned spins between half-filled Ni e_g and empty Mn e_g orbitals as expected in an extended Kugel-Khomskii model.[20,27] The superexchange path is active via the O $2p$ orbitals giving rise to a residual moment on the oxygen sites. The trend of the exchange parameters with changing R is reported in Table I.[28] In-plane exchange interactions between Mn sites are negligible compared to Ni sites. The ratio between the antiferromagnetic next-nearest-neighbor (NNN), $J^{NNN}_{\parallel(Ni\text{-}Ni)}$ and FM NN $J^{NN}_{\parallel(Ni\text{-}Mn)}$ interactions increases and explains the stabilization of E*-type magnetic structure: a frustrated ↑-↑-↓-↓ Ising-type spin chain in ab planes.[1,29] Magnetic couplings changed by intercalation of rare earth with smaller ionic radius gives the possibility to achieve a polar state in RNMO. We recall that the E-type magnetic structure is known to produce large polarization along the short b axis due to the noncentrosymmetric collinear spin arrangement which breaks the inversion symmetry in $RMnO_3$ and $RNiO_3$.[1,30–33]

There is an interesting similarity between the results presented here and the phenomena observed in the undoped

TABLE I. Values of the exchange interactions, J_{ij} (in meV/μ_B^2), for R_2NiMnO_6 (RNMO) with rare earths R=La, Sm, and Y: $J^{NNN}_{\parallel(Ni\text{-}Ni)}$, $J^{NNN}_{\parallel(Mn\text{-}Mn)}$, $J^{NN}_{\perp(Ni\text{-}Mn)}$, and $J^{NN}_{\parallel(Ni\text{-}Mn)}$ denote the in-plane Ni-Ni second-nearest neighbor, in-plane Mn-Mn second-nearest neighbor, out-of-plane Ni-Mn nearest-neighbor and in-plane Ni-Mn nearest-neighbor exchange constants, respectively. The ratio (Q) between $J^{NNN}_{\parallel(Ni\text{-}Ni)}$ and $J^{NN}_{\parallel(Ni\text{-}Mn)}$ is reported in the last column.

R	$J^{NNN}_{\parallel(Ni\text{-}Ni)}$	$J^{NNN}_{\parallel(Mn\text{-}Mn)}$	$J^{NN}_{\perp(Ni\text{-}Mn)}$	$J^{NN}_{\parallel(Ni\text{-}Mn)}$	Q
La	−100	3	44	47	2.13
Sm	−72	3	27	25	2.88
Y	−57	2	11	12	4.75

manganites $R\mathrm{MnO}_3$.[34,35] In the $R\mathrm{MnO}_3$, one finds a sequence of transitions from an A-type AFM (for R=La, Sm) to a spin-spiral (R=Tb, Dy) and finally to an E-type state (R=Ho). While the A-type phase is paraelectric, both the spin-spiral and the E-type phases are ferroelectric. In the case of double-perovskites RNMO, one starts with a FM state for R=La, which differs from LaMnO_3 only in the c-axis coupling. We predict that YNMO is E*-type AFM and supports a finite macroscopic polarization similar to the case of HoMnO_3. The other difference between the $R\mathrm{MnO}_3$ and the RNMO family is the existence of charge ordering in the latter. Since we do not consider noncollinear states, we cannot rule out the possibility of spin-spiral states. We believe that the possibility to find spin-spiral state is suppressed in the present case due to the anisotropic NNN hoping between Ni-Ni, which strongly favors the E*-type state. Nevertheless, if spin-spiral states indeed exist for some members of the family RNMO, these will very likely turn out to be ferroelectric much like the TbMnO_3 and DyMnO_3. Following the change in effective exchange parameters J_{ij} in Table I, one expects a reduction in transitions temperatures, similar to the case in $R\mathrm{MnO}_3$. Taking into account the difference between magnetic moments at Ni and Mn sites, we estimate the T_C in LNMO to be ~330 K, very close to the experimental value of 280 K. Comparing the energies of FM and E*-type phases, we expect the transition temperatures for R=Sm (R=Y) to be a factor of 2 (10) lower than that for R=La.

IV. MODEL HAMILTONIAN ANALYSIS

In order to understand the transition from the FM to the E*-type magnetic state at a more microscopic level, we analyze the following two-band model Hamiltonian[36,37] for the double perovskites:

$$
\begin{aligned}
H = & -\sum_{(ij)\sigma}^{\alpha\beta} t_{\alpha\beta}^{ij}(c_{i\alpha\sigma}^{\dagger}c_{j\beta\sigma} + \mathrm{H.c.}) + \sum_i \epsilon_i n_i + U\sum_{i,\alpha} n_{i\alpha\uparrow}n_{i\alpha\downarrow} \\
& + (U' + J_H)\sum_i n_{ia\uparrow}n_{ib\downarrow} + n_{ib\uparrow}n_{ia\downarrow} + (U' - J_H)\sum_i n_{ia\uparrow}n_{ib\uparrow} \\
& + n_{ia\downarrow}n_{ib\downarrow} - J_H \sum_{i\in \mathrm{Mn}} \mathbf{S}_i \cdot \boldsymbol{\sigma}_i + \lambda \sum_i (Q_{xi}\tau_{xi} + Q_{zi}\tau_{zi} + Q_{bi}n_i) \\
& + H_{el}. \qquad (1)
\end{aligned}
$$

Here, $c_{i\alpha\sigma}$ and $c_{i\alpha\sigma}^{\dagger}$ are annihilation and creation operators for electrons with spin σ in the e_g orbital $\alpha \in \{x^2-y^2(a), 3z^2-r^2(b)\}$. $t_{\alpha\beta}^{(ij)}$ denotes the hopping amplitudes between the two e_g orbitals on NN and NNN sites. The NN Ni-Mn hopping is given by[38] $t_{11}^x = t_{11}^y \equiv t$, $t_{22}^x = t_{22}^y \equiv t/3$, $t_{12}^x = t_{21}^x \equiv -t/\sqrt{3}$, and $t_{12}^y = t_{21}^y \equiv t/\sqrt{3}$, where x and y mark the spatial directions. The NNN hoppings are parameterized by t' such that $t_{\alpha\beta}^{\mathrm{NNN}} = t' t_{\alpha\beta}^{\mathrm{NN}}$.[39] ϵ_i denotes the on-site energy, and, guided by the electronic structure shown in Fig. 1, we set $\epsilon_i(\mathrm{Mn/Ni}) = \pm\Delta$. J_H denotes the Hund's rule coupling between the e_g electrons and U' (U) is inter (intra)band Hubbard repulsion with $U = U' + 2J_H$. Since the Mn sites have a half-filled t_{2g} level, an additional Hund's rule coupling between the Mn t_{2g} and the Mn e_g is included. The $\boldsymbol{\sigma}_i$ denotes the electronic spin operator defined as $\sigma_i^{\mu} = \Sigma_{\sigma\sigma'}^{\alpha} c_{i\alpha\sigma}^{\dagger} \Gamma_{\sigma\sigma'}^{\mu} c_{i\alpha\sigma'}$, where Γ^{μ} are the Pauli matrices. λ denotes the strength of the electron-lattice coupling. Q_{xi}, Q_{zi} are the Jahn-Teller (JT) distortions which are very weak compared to the breathing mode (BM) distortions Q_{bi}. The $\tau_{xi} = \Sigma_{\sigma}(c_{ia\sigma}^{\dagger}c_{ib\sigma} + c_{ib\sigma}^{\dagger}c_{ia\sigma})$ and $\tau_{zi} = \Sigma_{\sigma}(c_{ia\sigma}^{\dagger}c_{ia\sigma} - c_{ib\sigma}^{\dagger}c_{ib\sigma})$ are the orbital pseudospin operators for the e_g orbitals, and the elastic energy for the distortions is included as $H_{el} = (1/2)(Q_{xi}^2 + Q_{zi}^2 + Q_{bi}^2)$. Any deviation from collinear spin arrangements is neglected. All energies are measured in units of hopping parameter t, which can be estimated as $t \sim 0.2$ eV from the e_g bandwidth.

Ideally, one should also include in the model the hopping between Mn t_{2g} and Ni e_g orbitals. However, this will lead to a much more complex five-orbital model. Therefore, in order to retain the simplicity of the analysis we ignore the hopping between t_{2g} and e_g orbitals. Moreover, we believe that the qualitatively important term is the hopping between NNN Ni e_g orbitals, which has been explicitly included. Additionally, since the c-axis magnetic coupling remains ferromagnetic in nature, we consider only a two-dimensional (2D) model which captures all the relevant effects occurring in the in-plane parameters as inferred from the DFT data.

In spite of employing the simplifications discussed above, the model Hamiltonian is rather involved with a large number of parameters. We identify the key parameters of the model using inputs from DFT results. An important feature from DFT calculations is the increase in the relative strength of the NNN respect to the NN interactions as R changes from La to Y (see Table I). Therefore, we focus on this variation, keeping the other model parameters fixed to reasonable values guided by the DFT results.[20] A staggered pattern of the BM distortions with $Q_{bi} = Q_b e^{i(\pi,\pi)\cdot \mathbf{r}_i}$ is assumed following the DFT results discussed earlier. A weak JT distortion is also considered in order to test the robustness of the results. We analyze the model Hamiltonian by employing a Hartree-Fock decoupling of the interaction terms; replacing $n_{i\alpha\uparrow}n_{i\alpha\downarrow}$ by $\langle n_{i\alpha\uparrow}\rangle n_{i\alpha\downarrow} + n_{i\alpha\uparrow}\langle n_{i\alpha\downarrow}\rangle - \langle n_{i\alpha\uparrow}\rangle\langle n_{i\alpha\downarrow}\rangle$, etc. The resulting model is solved self-consistently by iterative numerical diagonalization on a two-dimensional Ni-Mn square lattice starting from different possible magnetic states, and the energies of the converged states are compared to find the ground state. In Fig. 2, we show the total energy per lattice site as a function of the ratio t' between the NNN and the NN hopping strengths. Panel (a) corresponds to the absence of JT distortions while weak JT distortions are present for the results in panel (b). The figure demonstrates that it is indeed possible to drive a transition from a ferromagnetic to an E*-type state by increasing the NNN hopping parameter. JT distortions work in favor of the E*-type state as the t' required for the FM to E*-type transition reduces upon increasing Q_x [see Fig. 2(b)].

V. FERROELECTRIC POLARIZATION

Using the BP approach, we evaluate the first-principles electric polarization P (Ref. 40) for YNMO. The purely electronic contribution to polarization, P_{ele}, can be calculated by imposing the E*-type magnetic structure in the centrosymmetric crystal structure with $P2_1/n$ symmetry, leading to

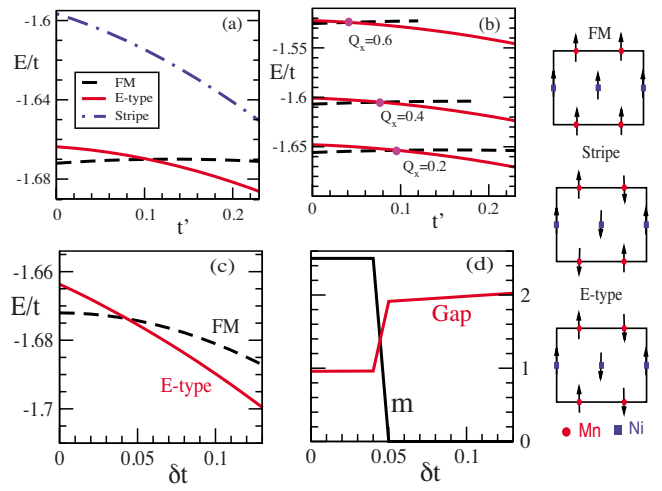

FIG. 2. (Color online) Total energy as a function of the ratio t' of the NNN to the NN hopping parameters, (a) in the absence and (b) in the presence, of JT distortions. The E-type state (equivalent to E* since the model is 2D) becomes lower in energy with increasing t' in both cases. The other model parameters are $\Delta=2$, $U'=4$, $J_H=0.5$, $\lambda=1$, $Q_z=0$, and $Q_b=1$. (c) Total energy as a function of δt for $\Delta=2.0$, $J_H=0.5$, $Q_x=0$, and $U'=4$. (d) Energy gap in the DOS and the net magnetization as a function of δt. All energies are measured in units of hopping parameter $t\sim 0.2$ eV.

$P_{ele}=0.75\ \mu C/cm^2$ along the b axis. The checkerboard pattern due to Ni^{2+} and Mn^{4+} valence in the monoclinic $P2_1/n$ crystal structure leads to the BM distortions of the NiO_3 and MnO_3 octahedra, which contain three inequivalent oxygen atoms (O_1 out of plane and O_2, O_3 in plane) with corresponding Ni-O-Mn (Ni-O_2-Mn and Ni-O_3-Mn) angles differing slightly due to the monoclinic distortion of the unit cell [see Fig. 3(a)]. The E*-type magnetic order further lowers the crystal symmetry to $P2_1$. The magnetic order couples to the lattice and influences the ionic positions and the electronic charge distribution, leading to a decrease in the electronic contribution with respect to the purely electronic term calculated for the centrosymmetric crystal structure. However, the total polarization increases with respect to the centrosymmetric crystal structure due to the ionic contribution: $P_{YNMO}=2.50\ \mu C/cm^2$ ($P_{ele}=0.51\ \mu C/cm^2$, $P_{ionic}=1.99\ \mu C/cm^2$). The exchange energy in the $P2_1$ symmetry is minimized: (i) by increasing (decreasing) the distance between ↑-↑(↑-↓) along the ↑-↑-↓-↓ spin chains [see d′, d″ in Fig. 3(b)], which are identical in the original $P2_1/n$ symmetry [see d in Fig. 3]; (ii) by further splitting from a magnetic point of view of the oxygen ions into four inequivalent sites [see Ni-$O_{2'}$-Mn, Ni-$O_{2''}$-Mn and Ni-$O_{3'}$-Mn, Ni-$O_{3''}$-Mn in Fig. 3(b)]. The inequivalent oxygen atoms $O_{2'}$, $O_{2''}$ and $O_{3'}$, $O_{3''}$ are charge polarized with local dipole moments leading to a net polarization developing along the b axis. The magnetic mechanism illustrated here has been found to be active also in multiferroic $RNiO_3$.[31] Details of the optimized structures for RNMO are given in Table II. The Ni-O-Mn angles decrease with the ionic radius R from La to Y, leading to a reduction in the effective overlap between NN Ni and Mn sites. This behavior explains qualitatively the change in the magnetic ground states upon changing the rare-earth ions similar to the observations in $RMnO_3$.[34]

TABLE II. Details of optimized ionic structures within E*-type (above) and ferromagnetic (below) structures. Please see Fig. 3 for notations.

R	d′	d″	N-$O_{2'}$-M	N-$O_{2''}$-M	N-$O_{3'}$-M	N-$O_{3''}$-M
La	3.888 Å	3.874 Å	155.66°	159.63°	155.92°	159.50°
Sm	3.811 Å	3.843 Å	151.84°	148.55°	151.70°	149.35°
Y	3.814 Å	3.776 Å	147.70°	144.68°	147.98°	145.68°

R	d	N-O_2-M	N-O_3-M
La	3.881 Å	158.06°	158.37°
Sm	3.827 Å	150.48°	150.89°
Y	3.795 Å	146.31°	147.0°

The ionic displacements from the centrosymmetric to the ferroelectric ionic state are such that all the ions contribute to the final polarization P. Larger displacements are found for Ni and O ions, excluding the possibility that P is driven by A-site cations only as in Bi-based multiferroic systems.[41]

To conclude our analysis, we compare the values of P_{YNMO} calculated within the BP approach and the so-called point charge model (PCM). We find $P^{PCM}_{YNMO}=1.64\ \mu C/cm^2$, i.e., very close to the one calculated by DFT taking into account quantum electronic effects. We deduce that the electronic rearrangement of the charge due to the symmetry breaking is small. An interesting outcome from DFT calculations can also be the deviation of the Born effective

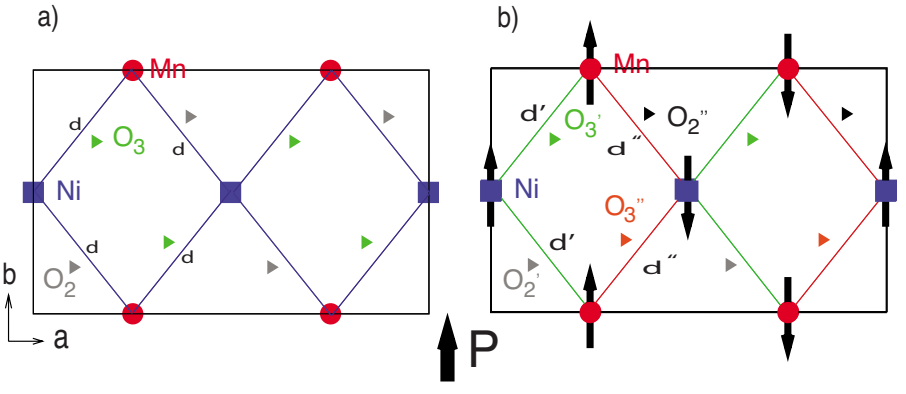

FIG. 3. (Color online) In-plane arrangement of the ions and their relative distances in the unit cell in (a) $P2_1/c$ and (b) $P2_1$ symmetry. Arrows indicate the magnetic spin ordering in the E*-type magnetic structure.

charges (BECs) from their nominal valencies looking at the (2,2) components:[42] $Z^*_{Ni}=1.9e, Z^*_{Mn}=4.85e$, $Z^*_{O_{3'}}=-2.87e$, $Z^*_{O_{2'}}=-2.0e$, $Z^*_{O_{3''}}=-3.65e$, $Z^*_{O_{2''}}=-2.76e$ (for the labeling of the oxygen sites see Fig. 3). The BEC are consistent with the inequivalence of oxygen sites and they are rather close to the nominal valences, providing a simple ionic picture of the chemical bonds in YNMO. In our analysis of the BEC, we did not consider the full tensor structure for the Z^* for all the atoms and assumed the (2,2) component to be most relevant one for multiferroicity. We calculated the electical polarization P also for SNMO and LNMO with imposing E^*-type magnetic structure using BP and PCM: $P^{PCM}_{SNMO}=1.69\ \mu C/cm^2$, $P^{BP}_{SNMO}=2.77\ \mu C/cm^2$, $P^{PCM}_{LNMO}=1.80\ \mu C/cm^2$, and $P^{BP}_{LNMO}=2.87\ \mu C/cm^2$. Note that the value of P in LNMO is larger than in YNMO, similar to what happens in E-type manganites.[25]

VI. DISCUSSIONS AND CONCLUSIONS

Finally, we demonstrate using the model Hamiltonian that an external electric field can induce a magnetic transition in this system. The main effect of an external electric field is to change the on-site energies of the oxygen, which enter in deriving the hopping parameters used in the model. To leading order the hoppings between Mn d and Ni d via the O $2p$ orbitals are $\propto t^2_{pd}/\Delta_{pd}$. Due to the inequivalence of bridging oxygens ($O_{2'}$ and $O_{2''}$ in Fig. 3), an external electric field makes Δ_{pd} and hence the d-d hopping parameters staggered. We use a parameter δt as a measure of this modulation, such that the hopping in both x and y direction are spatially staggered $(1\pm\delta t)t^{NN}_{\alpha\beta}$. Presence of an electric field (modeled as parameter δt) leads to a change in the magnetic ground state of the system from a FM to the E^*-type, as seen in Fig. 2(c). Figure 2(d) shows the discontinuous change in the total magnetization and the gap in the DOS across this transition. The jump observed in the magnitude of the gap is consistent with the DFT values for the two magnetic phases (see Fig. 1).

In conclusion, we have performed density-functional theory and model calculations to elucidate the possibility to find novel multiferroics in rare-earths R_2NiMnO_6 double perovskites. The magnetic state changes from a FM (R=La) to an E^*-type (R=Y): the later being well known to assist in ferroelectricity. Calculations on a two-band model combined with inputs from DFT calculations describe this magnetic transition. $Y_2NiMnO6$ is shown to be polar in its magnetic ground state with an intrinsic polarization comparable with other magnetically driven ferroelectrics.[43–46] We further show that an external electric field can change the magnetic ordering from FM to E^*-type leading to a flip from a nonpolar state with finite magnetization to a polar state with zero net magnetic moment: a major effect that is of interest for electronic devices. Similarly, an external magnetic field can allow for a switching between polar and nonpolar states. A similar switching of polarization with magnetic field has been reported recently for other multiferroic oxides with the potential of being a room-temperature device.[47] An order of magnitude estimate for the strength of field required to change from polar to nonpolar state can be obtained by considering the energy difference of these states. Assuming the hopping parameter $t\sim 0.2$ eV, we find that a magnetic field ~ 14 T would be required to make this flip. We should however comment that this is only a zeroth order estimate since it neglects the presence of defects, domain-wall dynamics, pinning effects, etc., by which the actual switching process in real materials is strongly affected. Nevertheless, we suggest further experimental investigations to test our theoretical predictions.

ACKNOWLEDGMENTS

We thank T. Fukushima and K. Yamauchi for stimulating discussions. This work is supported by Stichting FOM, NCF, and NanoNed. The research leading to part of these results has received funding from the European Research Council under the European Community Seventh Framework Program (FP7/2007-2013)/ERC under Grant Agreement No. 203523-BISMUTH. Computational support from CASPUR and SARA Supercomputing Centers are gratefully acknowledged.

[1] S. W. Cheong and M. Mostovoy, Nature Mater. **6**, 13 (2007).
[2] R. Ramesh and N. A. Spaldin, Nature Mater. **6**, 21 (2007).
[3] W. Eerenstein, N. D. Mathur, and J. F. Scott, Nature (London) **442**, 759 (2006).
[4] G. A. Smolensky and A. I. Agranovskaya, Zh. Tekh. Fiz. **28**, 1491 (1958).
[5] G. A. Smolensky, A. I. Agranovskaya, S. N. Popov, and A. V. Isupov, Zh. Tekh. Fiz. **28**, 2152 (1958).
[6] E. Ascher, H. Rieder, H. Schmid, and H. Stossel, J. Appl. Phys. **37**, 1404 (1966).
[7] N. A. Hill, J. Phys. Chem. B **104**, 6694 (2000).
[8] I. E. Dzyaloshinskii, Zh. Eksp. Teor. Fiz. **37**, 881 (1959).
[9] N. D. Astrov, Zh. Eksp. Teor. Fiz. **38**, 984 (1960).
[10] D. L. Fox and J. F. Scott, J. Phys. C **10**, L329 (1977).
[11] D. L. Fox, D. R. Tilley, J. F. Scott, and H. J. Guggenheim, Phys. Rev. B **21**, 2926 (1980).
[12] C. J. Fennie, Phys. Rev. Lett. **100**, 167203 (2008).
[13] M. H. Lente, J. D. S. Guerra, G. K. S. de Souza, B. M. Fraygola, C. F. V. Raigoza, D. Garcia, and J. A. Eiras, Phys. Rev. B **78**, 054109 (2008).
[14] G. M. Rotaru, B. Roessli, A. Amato, S. N. Gvasaliya, C. Mudry, S. G. Lushnikov, and T. A. Shaplygina, Phys. Rev. B **79**, 184430 (2009).
[15] R. Pirc, R. Blinc, and J. F. Scott, Phys. Rev. B **79**, 214114 (2009).
[16] M. Fechner, S. Ostanin, and I. Mertig, Phys. Rev. B **80**, 094405 (2009).
[17] Our E^* differ from the conventional E-type by the out-of-plane coupling: FM in E^* and AFM in E.
[18] C. L. Bull, D. Gleeson, and K. S. Knight, J. Phys.: Condens.

Matter **15**, 4927 (2003).
[19] K. Asai, H. Sekizawa, and S. Iida, J. Phys. Soc. Jpn. **47**, 1054 (1979).
[20] H. Das, U. V. Waghmare, T. Saha-Dasgupta, and D. D. Sarma, Phys. Rev. Lett. **100**, 186402 (2008).
[21] S. F. Matar, M. A. Subramanian, A. Villesuzanne, V. Eyert, and M. Whangbo, J. Magn. Magn. Mater. **308**, 116 (2007).
[22] G. Kresse and J. Furthmüller, Phys. Rev. B **54**, 11169 (1996).
[23] J. P. Perdew, K. Burke, and M. Ernzerhof, Phys. Rev. Lett. **77**, 3865 (1996).
[24] N. S. Rogado, J. Li, A. W. Sleight, and M. A. Subramanian, Adv. Mater. **17**, 2225 (2005).
[25] K. Yamauchi, F. Freimuth, S. Blugel, and S. Picozzi, Phys. Rev. B **78**, 014403 (2008); Y. Zhang, H. J. Xiang, and M.-H. Whangbo, *ibid.* **79**, 054432 (2009).
[26] In order to avoid any additional parameter which could make the discussion of the trends more difficult, we do not employ a GGA+U approach. Note that also in rare-earth manganites bare GGA reproduces the correct magnetic ground states (Ref. 25).
[27] K. I. Kugel ans D. I. Khomskii, Sov. Phys. Usp. **25**, 231 (1982).
[28] The J_{ij} values might be affected by details of exchange-correlation potential (GGA vs LDA, addition or not of Hubbard-type correction, etc). However, trends—of primary interests here—are expected not to be affected.
[29] M. E. Fisher and W. Selke, Phys. Rev. Lett. **44**, 1502 (1980).
[30] S. Picozzi, K. Yamauchi, B. Sanyal, I. A. Sergienko, and E. Dagotto, Phys. Rev. Lett. **99**, 227201 (2007).
[31] G. Giovannetti, S. Kumar, D. Khomskii, S. Picozzi, and J. van den Brink, Phys. Rev. Lett. **103**, 156401 (2009).
[32] J. J. Betouras, G. Giovannetti, and J. van den Brink, Phys. Rev. Lett. **98**, 257602 (2007).
[33] J. van den Brink and D. Khomskii, J. Phys.: Condens. Matter **20**, 434217 (2008).
[34] T. Goto, T. Kimura, G. Lawes, A. P. Ramirez, and Y. Tokura, Phys. Rev. Lett. **92**, 257201 (2004).
[35] S. Kumar, J. van den Brink, and A. P. Kampf, Phys. Rev. Lett. **104**, 017201 (2010).
[36] J. van den Brink and D. Khomskii, Phys. Rev. Lett. **82**, 1016 (1999); J. van den Brink, G. Khaliullin, and D. Khomskii, *ibid.* **83**, 5118 (1999).
[37] D. V. Efremov, J. van den Brink, and D. I. Khomskii, Nature Mater. **3**, 853 (2004); G. Giovannetti, S. Kumar, J. van den Brink, and S. Picozzi, Phys. Rev. Lett. **103**, 037601 (2009).
[38] J. C. Slater and G. F. Koster, Phys. Rev. **94**, 1498 (1954).
[39] In principle, the structure of the NNN hopping matrix is different from that of the NN one but these details are not important for the effect we are interested in.
[40] R. D. King-Smith and D. Vanderbilt, Phys. Rev. B **47**, 1651 (1993); R. Resta, Rev. Mod. Phys. **66**, 899 (1994).
[41] J. B. Neaton, C. Ederer, U. V. Waghmare, N. A. Spaldin, and K. M. Rabe, Phys. Rev. B **71**, 014113 (2005).
[42] A. Filippetti and N. A. Spaldin, Phys. Rev. B **68**, 045111 (2003).
[43] T. Kimura, T. Goto, H. Shintani, K. Ishizaka, T. Arima, and Y. Tokura, Nature (London) **426**, 55 (2003).
[44] N. Hur, S. Park, P. A. Sharma, G. L. Ahn, S. Guha, and S.-W. Cheong, Nature (London) **429**, 392 (2004).
[45] G. Giovannetti and J. van den Brink, Phys. Rev. Lett. **100**, 227603 (2008).
[46] T. Lottermoser, T. Lonkai, U. Amann, D. Hohlwein, and J. Ihringer, Nature (London) **430**, 541 (2004).
[47] A. Kumar, G. L. Sharma, R. S. Katiyar, R. Pirc, R. Blinc, and J. F. Scott, J. Phys.: Condens. Matter **21**, 382204 (2009); M. Kumar, A. Srinivas, and S. V. Suryanarayana, Appl. Phys. Lett. **92**, 132913 (2008).